

## ORIGINAL ARTICLE

# Synthesis of $\text{Zn}_{0.5}\text{Ti}_{0.5}\text{NbO}_4$ microwave dielectric ceramics with $\text{Li}_2\text{O-B}_2\text{O}_3\text{-SiO}_2$ glass for LTCC application

Hongyu Yang  | Enzhu Li | Hongcheng Yang | Hongcai He | Ren S. Zhang

School of Microelectronics and Solid  
State Electronics, University of Electronic  
Science and Technology of China,  
Chengdu, People's Republic of China

**Correspondence**

Enzhu Li  
Email: lienzhu@uestc.edu.cn

**Funding information**

National Natural Science Foundation of  
China, Grant/Award Number: 51272035;  
Specialized Research Fund for the  
Doctoral Program of Higher Education of  
China, Grant/Award Number:  
20110185120004

**Abstract**

Single phase of dense ixiolite structure  $\text{Zn}_{0.5}\text{Ti}_{0.5}\text{NbO}_4$  (ZTN) microwave dielectric ceramics were synthesized at low temperature (850°C–900°C) *via* solid state reaction with small amount of  $\text{Li}_2\text{O-B}_2\text{O}_3\text{-SiO}_2$  (LBS) glass. There is a liquid phase generated by LBS at about 760°C, which significantly enhances the shrinkage and decreases the activation energy. And with the assistance of liquid phase, single phase of ZTN with orthorhombic structure is detected, sintering temperature of ceramics drops from 1125°C to 850°C and still maintain high relative density (>97%) with great microwave dielectric properties ( $\epsilon_r \sim 34.32$ ,  $Q \times f \sim 17740$  GHz). Ceramics with 0.5 wt. % LBS cannot be sintered and densified, and the lack of densification determines a lower dielectric constant, large dielectric loss, and undetectability of temperature coefficient of resonant frequency. With the increase in LBS, a dense structure can be formed, but the deterioration of performance should be mainly attributed to the variation in LBS glass content.

**KEYWORDS**

$\text{Li}_2\text{O-B}_2\text{O}_3\text{-SiO}_2$  (LBS) glass, low temperature sintering, low-temperature co-fired ceramic, microwave dielectric properties,  $\text{Zn}_{0.5}\text{Ti}_{0.5}\text{NbO}_4$  (ZTN)

## 1 | INTRODUCTION

Much attention has been paid to microwave dielectric ceramics due to their wide range of application, for instance, bluetooth, handheld communications devices, filters, resonators, signal transmission.<sup>1,2</sup> Fabrication of ceramics usually requires high sintering temperature (>1000°C), such as the commercial microwave dielectric materials of  $\text{BaO-TiO}_2$  (densification of  $\text{BaTi}_4\text{O}_9$  demands a high temperature of 1300°C),<sup>3,4</sup>  $\text{Ba}(\text{Zn}_{1/3}\text{B}_{2/3})\text{O}_3$  (sintering temperature of 1500°C–1650°C for  $\text{B} = \text{Nb}$ , 1500°C for  $\text{B} = \text{Ta}$ )<sup>5,6</sup>, and their suitable temperatures exceed 1300°C, which is very energy-consuming. For the sake of conserving energy, low-temperature co-fired ceramic (LTCC) technology emerges as the time requires, besides, LTCC plays an important role in passive integration, reducing circuit dimension, which can improve the flexibility of the design of circuits, however, LTCC application

demands a low sintering temperature for the co-firing with Ag and Cu electrodes (melting point of Ag, Cu is 961°C and 1083°C, respectively), the materials should also maintain great microwave dielectric properties, such as  $\text{Bi}_2\text{O}_3\text{-TiO}_2\text{-V}_2\text{O}_5$ , Bi-Li-Ta, and  $\text{BiVO}_4\text{-LaNbO}_4$  system studied by Zhou, the sintering temperature of ceramic can be decreased to 800°C and still maintain great properties.<sup>2,7–13</sup>

$\text{Zn}_{0.5}\text{Ti}_{0.5}\text{NbO}_4$  (ZTN) ceramics with a  $\alpha\text{-PbO}_2$ -related ixiolite structure has been studied due to its appropriate dielectric constant ( $\epsilon_r$ , 34 ~ 38), high quality factor ( $Q \times f$ , 35000 ~ 40000 GHz) and relative low sintering temperature (1100°C ~ 1200°C).<sup>14–16</sup> The sintering temperature is still too high, which restricts its practical use in the LTCC field, therefore, many studies have been implemented to form pure ZTN phase at a sintering temperature lower than 1000°C. The addition of oxides with low melting point into matrix materials is a classic method to reduce the sintering temperature. Zhou used  $\text{BaCu}(\text{B}_2\text{O}_5)$  and decreased the

temperature of ZTN to 950°C, but the formation of second phase  $\text{ZnNb}_2\text{O}_6$  ( $\epsilon_r \sim 25.1$ ) will decrease the dielectric constant according to the mixture rule,<sup>15</sup> Li prepared ZTN ceramics at 875°C with  $\text{Li}_2\text{O-ZnO-B}_2\text{O}_3$  glass, where the  $\text{ZnNb}_2\text{O}_6$  phase is also detected,<sup>17</sup> Tseng lowered the sintering temperature to 920°C, using ZnO, however, the ZnO phase coexisted with ZTN, it also has a negative effect on the dielectric constant and  $Q_{xf}$  value.<sup>18</sup> Among these research methods, the appearance of secondary phase is not beneficial to the development of dielectric properties, besides, low temperature sintering behavior of glass additives on the ceramic is not fully elaborated.

In our previous work,  $\text{Li}_2\text{O-B}_2\text{O}_3\text{-SiO}_2$  (LBS) glass has shown a great solubility in  $\text{Li}_2\text{O-Nb}_2\text{O}_5\text{-TiO}_2$  systems, it can be synthesized successfully at low temperature with good microwave dielectric properties.<sup>19</sup> Considering the great compatibility with  $\text{Nb}_2\text{O}_5$ -based system, in order to explore the application of ZTN ceramics in LTCC field, LBS glass was taken into consideration for low temperature sintering of ZTN ceramics. Considering pure ZTN ceramics cannot be directly synthesized under 1000°C, this work has adopted low melting oxides, called LBS glass, and managed to fabricate a single phase of ZTN ceramic at 850°C-900°C with high densification and great microwave dielectric properties, and discussed the effects of LBS on the crystal structure, microstructure and properties.

## 2 | EXPERIMENTAL

The solid-state method was used to synthesize ZTN ceramics from high purity raw materials ZnO,  $\text{TiO}_2$ ,  $\text{Nb}_2\text{O}_5$  powders (>99.9%). The starting powders were mixed together and ball-milled with zirconia balls in nylon jar under deionized water for 6 hours. Thereafter, the mixtures were dried and calcined at 1000°C for 3 hours. The sintering aid of LBS glass was fabricated from the high-purity powders of  $\text{Li}_2\text{CO}_3$ ,  $\text{H}_3\text{BO}_3$ , and  $\text{SiO}_2$  (38.82:55.30:5.88 wt. %). The batches were dry-milled 2 hours with  $\text{ZrO}_2$  and melted at 1400°C for 2 hours, the melt was quenched from a copper plate to form glass. Different amounts of LBS glass were added into the calcined ZTN powders and remilled for 6 hours. After drying in air, acrylic acid was added into the mix powders to form pellets (13 mm in diameter and 7 mm in thickness). The pellets were sintered at 850°C-900 °C for 4 hours in air with heating and cooling rates of 2°C/min.

The crystal structures of the specimens were tested by X-ray diffraction (XRD, DX-1000 CSC, Japan) with scanning angles  $2\theta$  of 20° to 80°, using Cu K $\alpha$  radiation. Rietveld refinement was used to refine the crystal structures and obtain important lattice parameters.<sup>20</sup> The microstructures of the samples were observed through scanning

electron microscopy (SEM, FEI Inspect F, the UK). The bulk density was determined by the Archimedes method, the theoretical density was calculated from the following equation:<sup>21</sup>

$$\rho_1 = \frac{n \times A}{V \times N} \quad (1)$$

$$\rho_{\text{theo}} = (W_1 + W_2) \left( \frac{W_1}{\rho_1} + \frac{W_2}{\rho_2} \right)^{-1} \quad (2)$$

where 1,2,  $n$ ,  $A$ ,  $V$ ,  $N$ ,  $W$  represents ZTN, LBS glass, number of atoms in the unit cell, atomic weight, volume of unit cell, Avogadro number and weight fraction, respectively. The relative densities of the composite ceramics were obtained from the following:<sup>21,22</sup>

$$\rho_{\text{relative}} = \frac{\rho_{\text{bulk}}}{\rho_{\text{theo}}} \quad (3)$$

The thermomechanical analyses (TMA) (Model DIL 420C, Netzsch, Germany) were used to get the shrinkage (under heating rate of 10°C/min) and  $\Delta L/L$  (under heating rate of 5-15°C/min) when the ceramics sintered to certain temperatures. The change in LBS glass on the surface of ZTN ceramics were determined by a sintering point testing device, which were sintered to 900°C with a heating rate of 5°C/min. The microwave dielectric properties were investigated by the Hakki-Coleman dielectric resonator method in the TE011 mode, using a network analyzer (HP83752A, the United States), the  $\tau_f$  value was estimated from the following formula, calculating the change between the resonant frequencies under 25°C and 85°C:

$$\tau_f = \frac{f_{85} - f_{25}}{f_{25} \times 60} \times 10^6 (\text{ppm}/^\circ\text{C}) \quad (4)$$

## 3 | RESULTS AND DISCUSSION

The shrinkage curves of ZTN samples under a sintering rate of 10 K/min with different amounts of LBS glass are shown in Figure 1A, ZTN ceramic, and that with 1 wt. % LBS addition sintered to certain temperatures by adopting three different sintering rates of 5-15 K/min, with shrinkage measured at various temperatures are shown in Figure 1B. Without LBS, the initial shrinkage temperature of ZTN ceramic is about 800°C and the shrinkage is only 5.67% at 1000°C. When small amount of LBS (0.5 - 2 wt. %) was added, the onset shrinkage temperature is decreased to 500°C and the shrinkage increases to 17.66% at most. With 2 wt. % LBS added, the shrinkage changes a little from 14.37% to 16.68% after 900°C. And with 3wt. % LBS added, the shrinkage remains almost the same after 900°C, indicating the samples have achieved densification at 900°C. The results verify LBS glass has the ability of

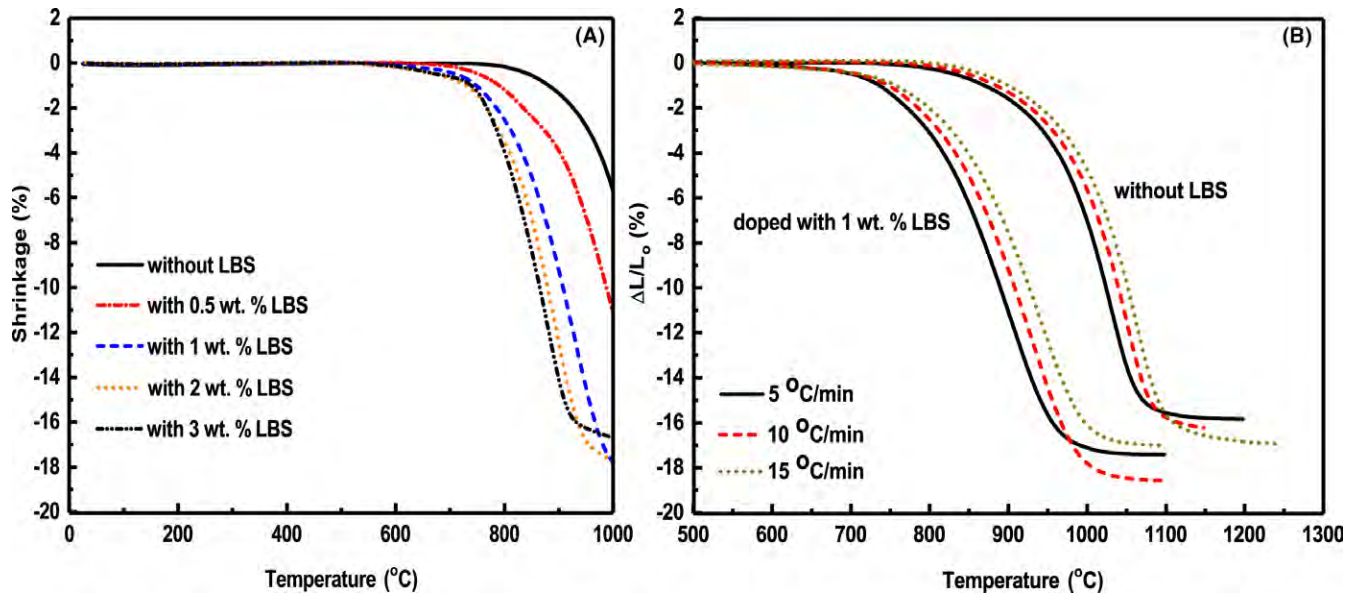


**FIGURE 1** A, Shrinkage curves of ZTN ceramics under a sintering rate of 10 K/min with different amount of LBS glass sintered from room temperature to 1000 °C. B, The shrinkage of ZTN ceramic and that with 1 wt. % LBS glass sintered at different sintering rates

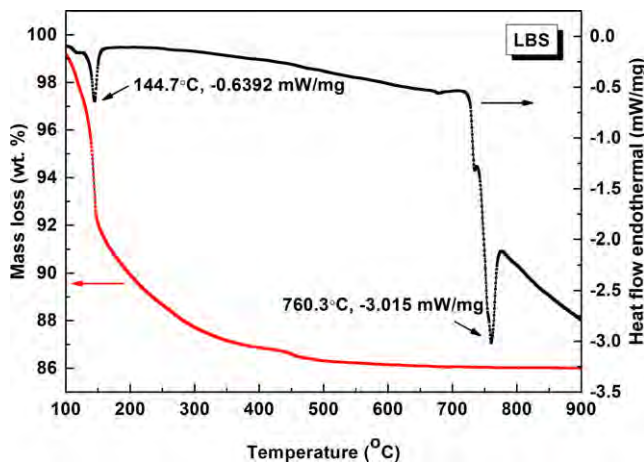


**FIGURE 2** DSC and TG curves of LBS glass

increasing the densification of ZTN ceramic at low sintering temperatures.

To study the melting points and wetting ability of LBS glass, DSC and TG curves of LBS glass are presented in Figure 2. During the heating process, the mass loss of LBS glass arrives at 12.93%, the two observable endothermic peaks around 144.7°C and 760.3°C. Here, 144.7°C might be the temperature of glass losing the crystal water, melting temperature of LBS glass is around 760.3°C.

The wetting behaviors of LBS glass on ZTN ceramic are shown in Figure 3. LBS glass is placed on the surface of ZTN substrate, before testing, ZTN sample was sintered at 1150°C to remove pores and improve densification. The volume of LBS does not change before 675°C, it shrinks

dramatically at 791°C, and melts into the ZTN ceramic at 795°C. It can be seen that the contact angle between the solid and liquid decreases along with the temperature, which illustrates a liquid phase that is generated by LBS glass and ZTN ceramics can be lubricated by the liquid phase.

For better insight into this liquid phase sintering mechanism, the  $\ln k$  ( $k$  refers to the sintering rate) as a function of  $1/T$  (temperature in Kelvin) is shown in Figure 4A-B, the shrinkage of 3, 6, 9, and 12% was considered for different heating rates at some certain temperatures. The activation energy ( $E_a$ ) between the two specimens were calculated, using the Arrhenius formula:<sup>23</sup>

$$\ln k = \frac{-E_a}{R} \left[ \frac{1}{T} \right] + \ln z \quad (5)$$

where  $E_a$  is the slope of the figure of  $\ln k$  against  $1/T$  multiplied by the gas constant,  $z$  is a constant value,  $R = 8.3145$  J/K/mol.

After measuring from the dilatometric curves, there is an average  $E_a$  of  $573.20 \pm 12.69$  kJ/mol for undoped LBS glass and an average  $E_a$  of  $345.86 \pm 12.63$  kJ/mol for ZTN with 1 wt. % LBS addition. These results show a relatively lower activation energy is required by doping with LBS glass, same results are found in the  $\text{CaO-Al}_2\text{O}_3\text{-SiO}_2$  system, the presence of the liquid phase is not to bring in new phases, besides, the more liquid phase, the lower the activation energy measured.<sup>23-25</sup> In the low temperature-sintering process of ZTN ceramic with LBS glass, shown in Figure 5, when the sintering temperature is higher than the melting temperature of glass, the formation of a liquid

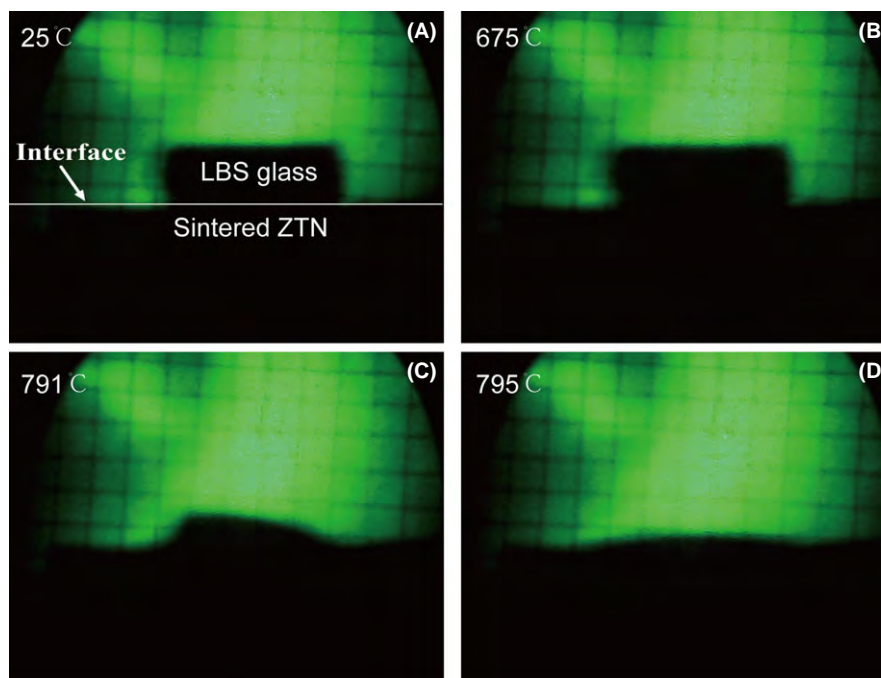


FIGURE 3 Wetting behaviors of LBS glass on the surface of ZTN substrate

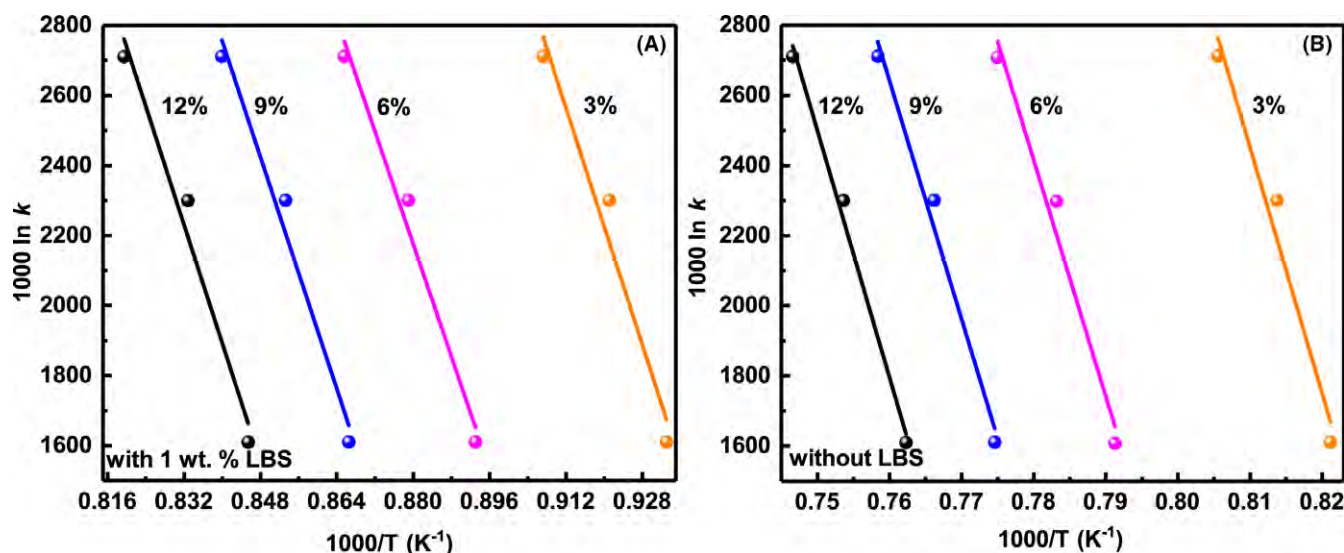


FIGURE 4 1000 ln k as a function of 1000/T at different shrinkages (A) without LBS glass; (B) with 1 wt. % LBS glass

phase wets the powders, at this condition, a capillary membrane will also be formed, which provides high pressure between powders, meanwhile the liquid phase lubricates powders, and the two driven forces accelerate the arrangement of powders, leading to densification.<sup>26</sup>

The X-ray diffractions of ZTN ceramics with different proportion of LBS glass sintered at 850°C - 900°C are shown in Figure 6A,B.

The diffraction peaks appearing in the sintered samples can be indexed to the orthorhombic structure  $\text{ZnTiNb}_2\text{O}_8$  (JCPDS # 48-0323), the relevant indices of crystallographic

planes are also marked, no secondary phase was detected, which means a single phase of ZTN has been successfully formed at low sintering temperature. To further study the influence of LBS glass on the structural parameters of ZTN phase, Rietveld refinement was used. The starting model of  $\text{ZnTiNb}_2\text{O}_8$  (ICSD # 40710) was chosen as reported by Baumgarte and Blachnik,<sup>27</sup> the reliability factor of the weighted pattern ( $R_{wp}$ ), reliability factor of weighted pattern ( $R_p$ ), and the goodness of fit ( $\chi^2$ ) should judge the reliability of the fitting results. The refined and calculated structural parameters are listed in Table 1.



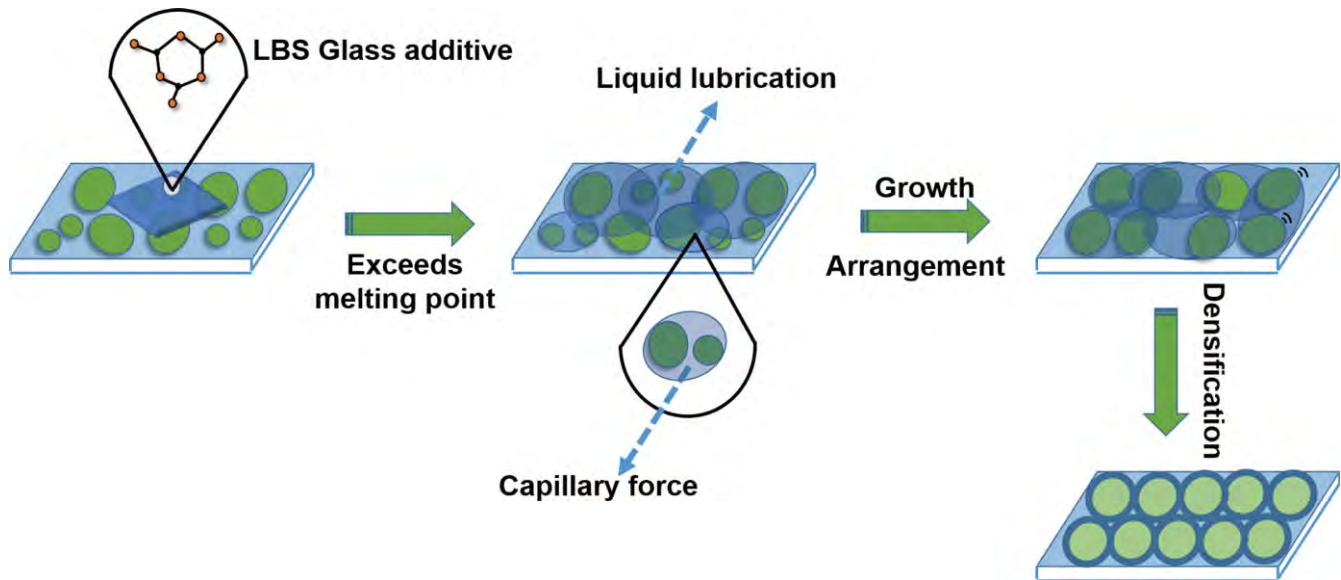


FIGURE 5 Schematic illustration of liquid phase sintering process

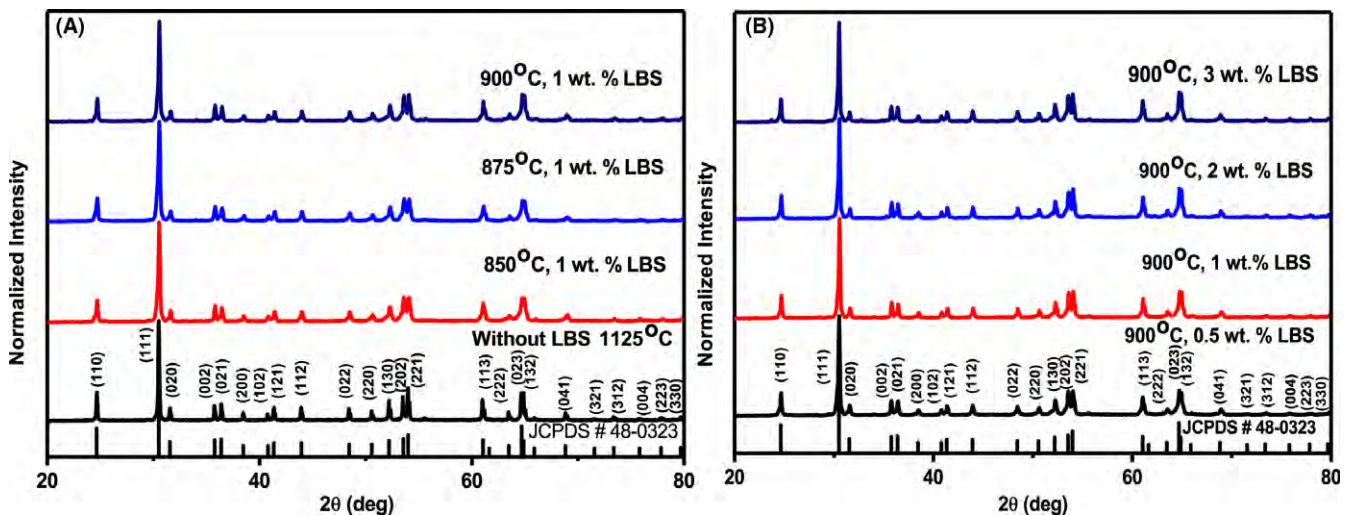


FIGURE 6 X-ray diffraction patterns of ZTN ceramics with different amount of LBS glass

When the samples sintered at 850 °C - 900°C with 1 wt.% LBS and 1125°C without LBS, the lattice parameters show a drop tendency, while these parameters change a little when sintered at 900°C with 0.5-3 wt. % LBS, which means LBS glass will not change the structural parameters too much.

The surfaces of ZTN ceramic sintered at 900°C with 0.5 – 3 wt. % LBS are shown in Figure 7A-D, the corresponding grain size distributions are presented in Figure 8.

The grain is very small and the grain size narrowly distributed in 0.1-1.0 μm at 0.5 wt. % LBS glass, which has an average value of 0.20 μm, the structure is porous, and the liquid phase appears. This phenomenon determines a lower densification. When the LBS glass content increases

to 1 wt. % and 2 wt. %, pores gradually disappear, liquid phase covers over the surface, besides, the grain size distribution steadily becomes wide, and the average grain increases from 0.28 μm to 1.28 μm. It is noticeable that there is not much change in the average grain size in 0.5 – 1 wt. % LBS, but the relative density increases dramatically, this is because the liquid phase fills the pores between grains, making the structure more densified. After 2 wt. % LBS added, the grains are clearly to be observed, grain boundary is also clear, but abnormal grain growth causes an increase of grain size, and its distribution is less than uniform.

The bulk density of the ceramic is shown in Figure 9 (a), the theoretical density of ZTN phase, that with 1 wt. %

**TABLE 1** Structural parameters of ZTN ceramics with 0 - 3 wt. % LBS glass after refinement

ST (°C)	850	875	900	900	900	900	1125
LBS (wt. %)	1	1	0.5	1	2	3	0
a (Å)	4.6868 (4)	4.6621 (4)	4.6647 (3)	4.6640 (3)	4.6639 (3)	4.6641 (3)	4.6680 (1)
b (Å)	5.6734 (3)	5.6457 (4)	5.6480 (3)	5.6477 (3)	5.6491 (3)	5.6487 (3)	5.6524 (1)
c (Å)	5.0262 (3)	5.0024 (3)	5.0054 (2)	5.0052 (2)	5.0051 (3)	5.0041 (2)	5.0073 (1)
$V_{\text{cell}}$ (Å <sup>3</sup> )	133.65	131.67	131.87	131.84	131.90	131.84	131.12
$\rho_1$ (g/cm <sup>3</sup> )	5.3059	5.3857	5.3776	5.3788	5.3776	5.3788	5.4083
$\rho_{\text{theo}}$ (g/cm <sup>3</sup> )	5.2431	5.3202	5.3446	5.3135	5.2499	5.1911	5.4083
$\rho_{\text{relative}}$ (%)	91.13	94.73	92.65	97.21	97.16	97.15	96.36
$R_{\text{wp}}$ (%)	11.41	11.38	11.47	11.81	12.37	11.43	10.30
$R_p$ (%)	8.64	8.62	8.52	9.01	9.41	8.70	7.97
$\chi^2$	1.983	2.209	2.147	2.187	2.205	1.946	2.125

ST,  $V_{\text{cell}}$ ,  $\rho_1$ ,  $\rho_{\text{theo}}$ ,  $\rho_{\text{relative}}$ ,  $R_{\text{wp}}$ ,  $R_p$ ,  $\chi^2$  refers to sintering temperature, Volume of unit cell, theoretical density of  $\text{Zn}_{0.5}\text{Ti}_{0.5}\text{NbO}_4$  phase, theoretical density of sintered samples, reliability factor of weighted pattern ( $R_{\text{wp}}$ ), reliability factor of weighted pattern ( $R_p$ ), and goodness of fit ( $\chi^2$ ), respectively.

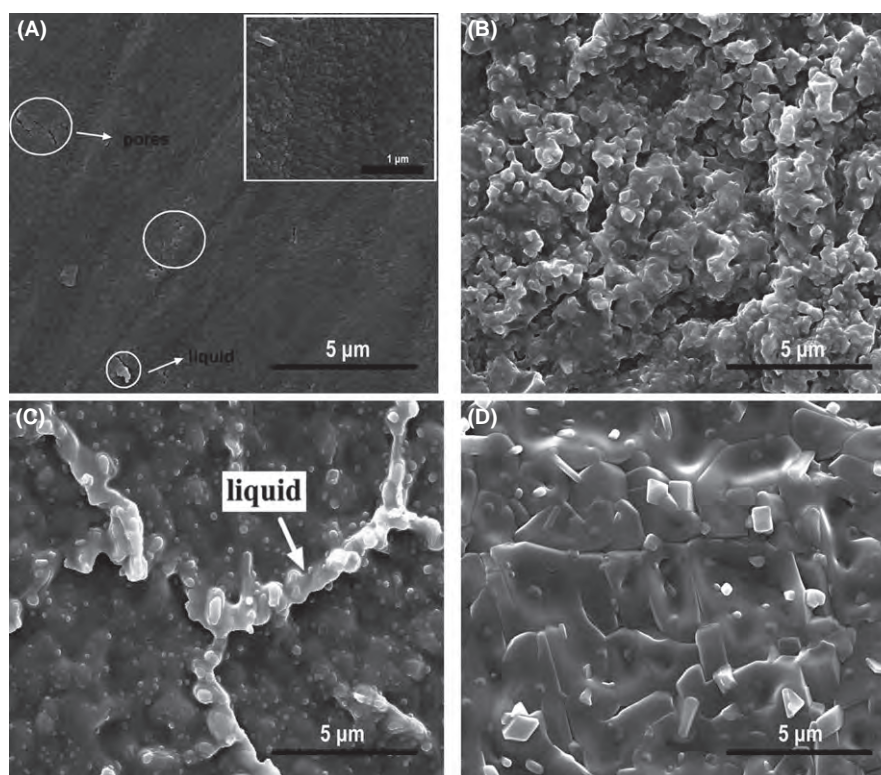


**FIGURE 7** Surface of ZTN ceramic with different amount of LBS glass sintered at 900°C (A) 0.5 wt. %, (B) 1 wt. %, (C) 2 wt. %, (D) 3 wt. %

LBS, and the relative density are shown in Figure 9B, the ceramic sintered at 1125°C without LBS is presented as the contrast experiment, the ceramic sintered at 900°C with 0.5 - 3 wt. % LBS is shown in Figure 9C.

From Figure 9A, the higher the sintering temperature, the lower LBS glass content required for achieving a maximum density (the ceramic gets a maximum density of 5.165 g/cm<sup>3</sup> at 900°C for 1 wt. % LBS glass), and with the

increase in LBS content, the bulk density increases to a certain value firstly and then drops, the decrease in the ceramic is attributed to the lower density of LBS glass (2.40 g/cm<sup>3</sup>).<sup>7</sup> From Figure 9B,C, the theoretical density of ZTN with LBS glass is lower than that without LBS, which is mentioned above, due to the lower density of LBS glass. The relative density of ceramic with 1 wt. % LBS (97.21%) is the largest, while, the relative density of

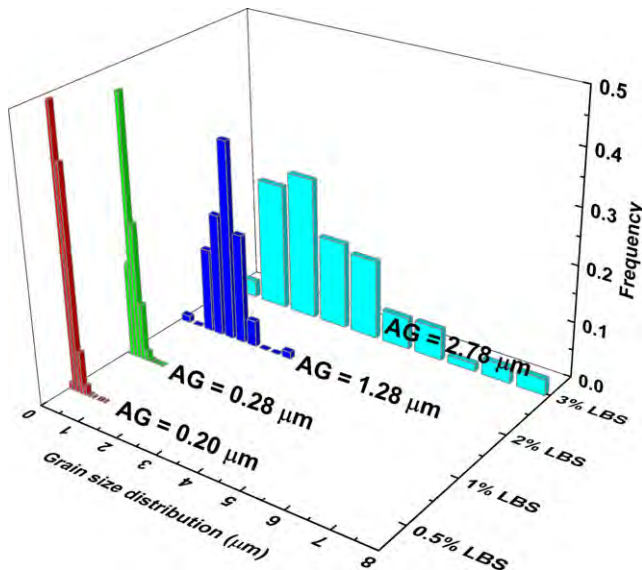


**FIGURE 8** Grain size distribution of ZTN ceramics sintered at 900°C with different amount of LBS glass (AG refers to the average grain size)

the ceramic sintered at 900°C with 0.5 - 3 wt. % LBS glass increases at first, and keep nearly steady after 1 wt. %, which means the ceramic can be sintered to the most compact at 900°C with 1 wt. % LBS.

The variations of  $\epsilon_r$  value of ZTN ceramics sintered at 850 °C - 900 °C with 0.5 – 3 wt. % LBS are shown in Figure 10 (a). As known, the  $\epsilon_r$  value is influenced by the dielectric polarizability, relative density, crystal structure, second phase, and the additives.<sup>22,28</sup> Since there is no second phase formed or change in crystal structure, and the dielectric polarizability of ZTN does not change, the relative density and the additives should be responsible for the variation in  $\epsilon_r$  value. For instance, the ceramic sintered at 900 °C with 0.5 wt. % LBS has the lowest dielectric constant of 29.7, this is because the ceramic is not sintered densified (92.65%), the lower relative density determines the lower  $\epsilon_r$  value, which also can be illustrated from the shrinkage curves (see Figure 1), after 1 wt. % LBS, the ceramic achieves a relative density (above 97%), the additive becomes the important reason influencing the  $\epsilon_r$  value.

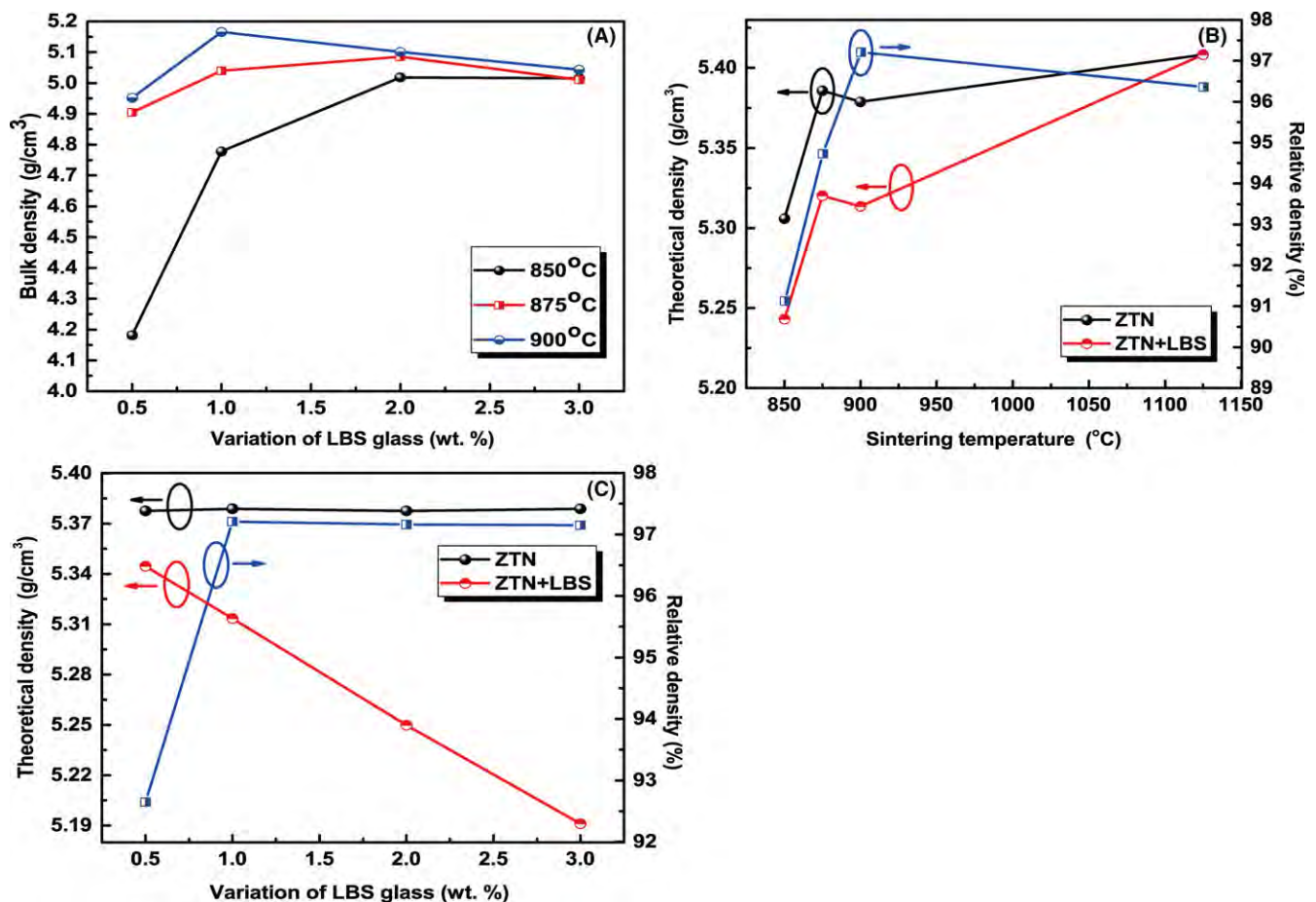


**FIGURE 9** Bulk density, theoretical density and relative density of the sintered samples



The influence of the additives can be followed by the additives mixing rules:<sup>15,29</sup>

$$\varepsilon^{-1} = V_1 \varepsilon_1^{-1} + V_2 \varepsilon_2^{-1} \text{ (serial mixing model)} \quad (6)$$

$$\varepsilon = V_1 \varepsilon_1 + V_2 \varepsilon_2 \text{ (parallel mixing model)} \quad (7)$$

$$\ln \varepsilon = V_1 \ln \varepsilon_1 + V_2 \ln \varepsilon_2 \text{ (logarithmic mixing model)} \quad (8)$$

where  $V_1$ ,  $V_2$  represents the volume fraction of ZTN and LBS glass,  $\varepsilon_1$  and  $\varepsilon_2$  values of ZTN and LBS glass are chosen as 36.35 and 7.58, respectively.

The calculated and measured  $\varepsilon_r$  values of the samples sintered at 900°C are shown in Figure 10B, due to lack of densification, the measured value is the minimum at 0.5 wt. %, thereafter it decreases, while the calculated  $\varepsilon_r$  values predicted from three models show the same decreased tendency, the Logarithmic mixing model presents the best predictability.

The variations of  $Q \times f$  values, packing fraction, average grain size and Q values are shown in Figure 11A-D.

The  $Q \times f$  values increases firstly and decrease at 850°C and 875°C, decrease monotonously at 900°C. Intrinsic loss and extrinsic loss are the reason for the change in dielectric loss. Intrinsic loss, caused by the lattice vibration, can be reflected from the packing fraction value. Extrinsic loss, influenced by the relative density, grain size, second phase, and the additives. The packing fraction can be calculated from the following:<sup>30</sup>

$$\text{Packing fraction} = \frac{V_{\text{ions}}}{V_{\text{cell}}} \quad (9)$$

$$V_{\text{ions}} = \frac{4}{3} \pi (r_{\text{Zn}^{2+}}^3 + r_{\text{Ti}^{4+}}^3 + 2 \times r_{\text{Nb}^{5+}}^3 + 8 \times r_{\text{O}^{2-}}^3) \quad (10)$$

where  $V_{\text{cell}}$  is obtained from the refined results, and because  $\text{Zn}^{2+}$ ,  $\text{Ti}^{4+}$ , and  $\text{Nb}^{5+}$  have the same coordinate

number (CN = 6), the ionic radii is chosen as 0.74, 0.605, and 0.64, respectively, for  $\text{O}^{2-}$ , the ionic radii is 1.36 (CN = 3) from Shannon's report.<sup>31</sup>

Since there are no changes of  $V_{\text{ions}}$ , the packing fraction is inversely proportional to the volume of unit cell. The volume of ZTN ceramic decreases from 850°C to 875°C with 1 wt. % LBS, and then increases, so the packing fraction shows the contrary variation, the minimum value at 850°C shows the larger dielectric loss, however the changes of the  $Q \times f$  values are small at 850°C-900°C with 1 wt. % LBS glass, which means the influence of packing fraction is not the main reason. While, the packing fraction changes a little when the ceramics sintered at 900°C with 0.5-3 wt. % LBS, so the decrease in  $Q \times f$  value is no longer determined by the intrinsic part, and since there is no second phase, the relative density is also high, the additives and average the grain size should be the main reasons affecting the  $Q \times f$  value. As seen from Figure 9, there is an increase in average grain size, however, the  $Q \times f$  value still decreases, so the large dielectric loss should originate from the LBS glass additive. Because the ceramics are measured at different frequency, so the Q value can reflect the change in dielectric loss, and the calculated Q value is obtained from the mixing rule:<sup>15</sup>

$$\frac{1}{Q} = \frac{V_1}{Q_1} + \frac{V_2}{Q_2} \quad (11)$$

where 1, 2 represents ZTN and LBS glass: ZTN ceramics with microwave dielectric properties:  $\varepsilon_r = 36.35$ ,  $\tan \delta = 1.38 \times 10^{-4}$ ,  $Q \times f = 40,156 \text{ GHz}$  (at 5.718 GHz),  $\tau_f = -68.76 \text{ ppm/}^\circ\text{C}$  and LBS from reference:  $\varepsilon_r = 7.58$ ,  $\tan \delta = 4.5 \times 10^{-3}$ ,  $\tau_f = -86 \text{ ppm/}^\circ\text{C}$ .<sup>7</sup>

The calculated Q values of the ceramics sintered at 900°C decrease along with the increase in LBS glass content, while with 1 wt. % LBS addition, the calculated Q

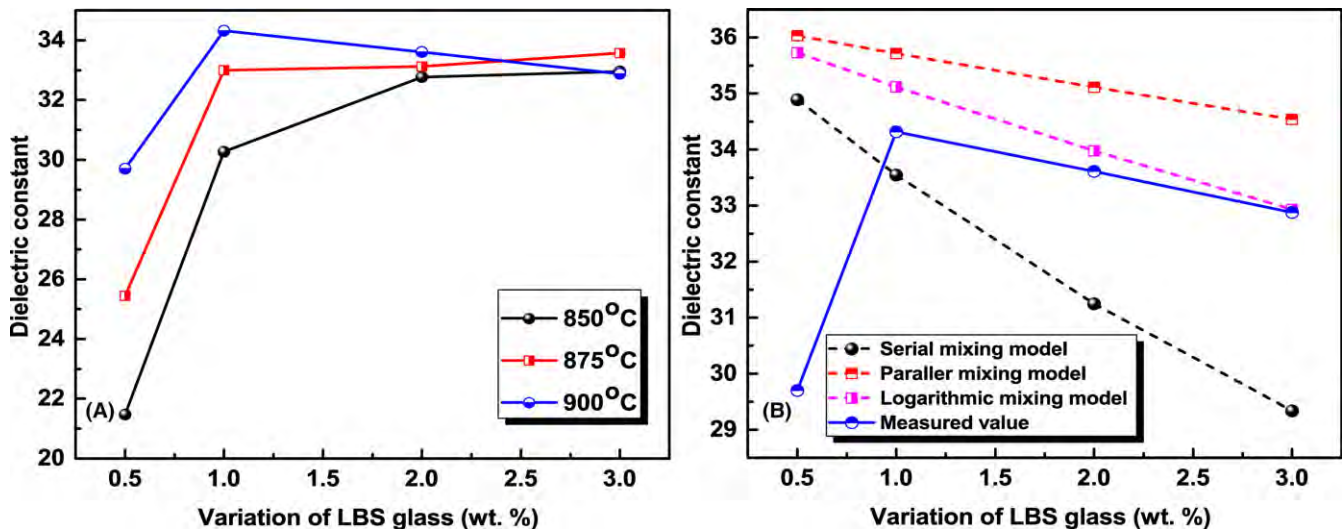


FIGURE 10 Measured dielectric constant of the sintered samples (A), and calculated dielectric constant from three different models (B)



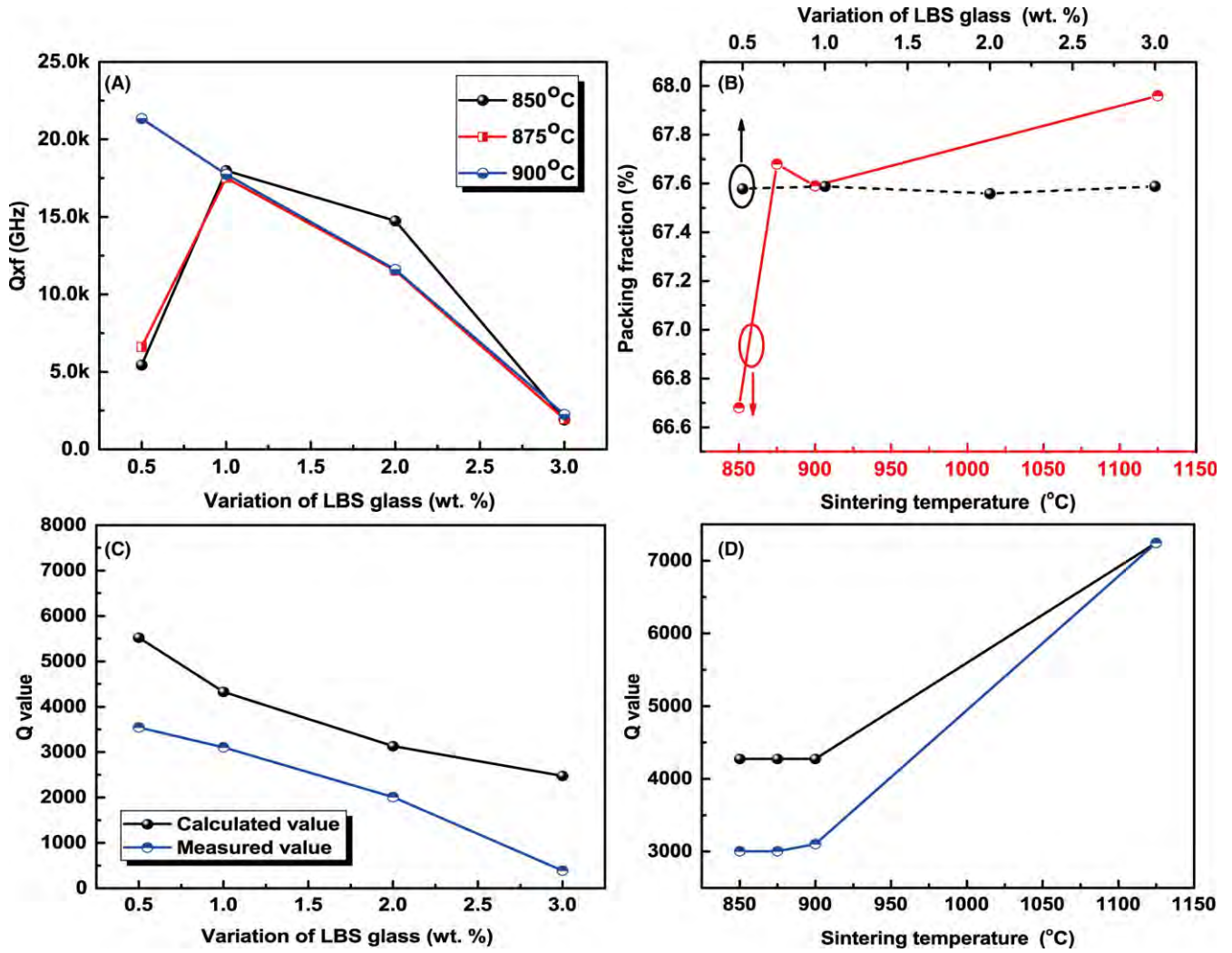


FIGURE 11 Measured  $Q_{xf}$  values of the sintered samples (A), calculated packing fraction (B), and calculated Q as functions of (C) LBS content (D) sintering temperature

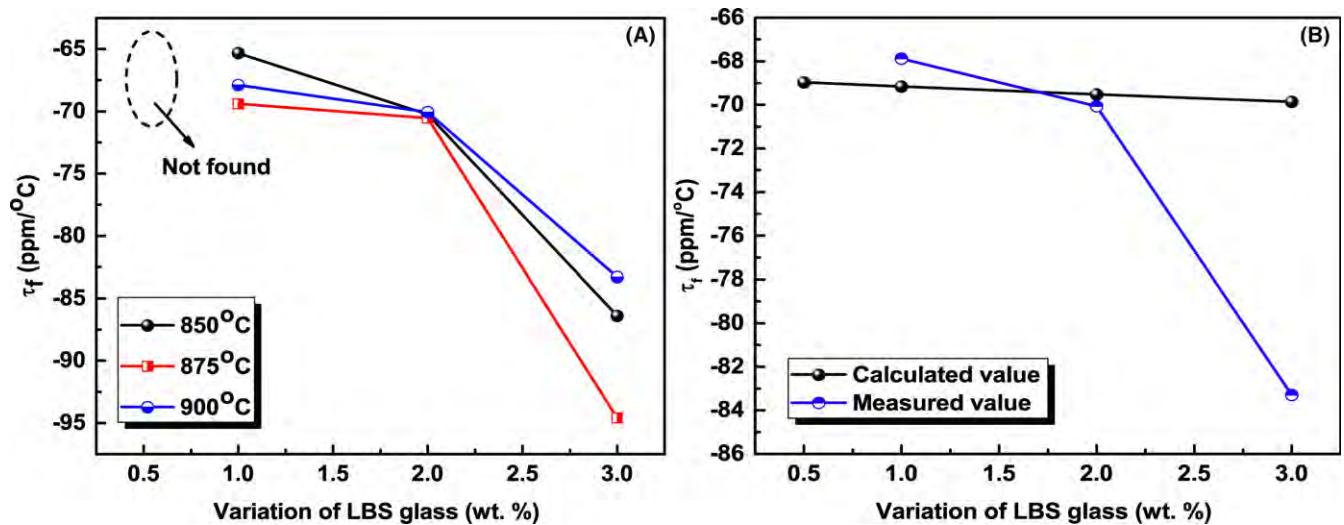


FIGURE 12 Measured and calculated  $\tau_f$  values of the sintered samples

value increases slightly from 850°C to 900°C. Both changes are similar to the calculated values. Therefore, it can be concluded the large dielectric loss is attributed to LBS glass content.

The variations of  $\tau_f$  values are shown in Figure 12A-B. The measured and calculated  $\tau_f$  values show a similar drop tendency. From previous reports, the crystal structure with a second phase, relative density, and the additive measure all of these have an impact on  $\tau_f$  values.<sup>22</sup> In our work, since the crystal structure is not change, the relative density of ceramics sintered at 900°C at 1 – 3 wt. % LBS is higher, and there is no second phase shown, the development of the  $\tau_f$  values rely on the content of LBS glass. The calculated  $\tau_f$  value can be obtained from the following:<sup>15</sup>

$$\tau_f = V_1\tau_{f1} + V_2\tau_{f2} \quad (12)$$

The calculated value decreases along with the increase in LBS amount, which is attributed to the negative value of LBS (-86 ppm/°C),<sup>8</sup> the variation in the calculated value is consistent with the measured value.

## 4 | CONCLUSION

The present work has successfully fabricated single phase of  $\text{Zn}_{0.5}\text{Ti}_{0.5}\text{NbO}_4$  ceramics at 850°C–900°C with small amounts of LBS glass. LBS has a slight impact on the structural parameters but a great deal on the grain size distribution, relative density, and microwave dielectric properties. With 1 wt. % LBS addition, a maximum relative density of 97.21% and optimal microwave dielectric properties ( $\epsilon_r = 34.32$ ,  $Q \times f = 17,740$  GHz,  $\tau_f = -67.88$  ppm/°C) can be obtained. The more LBS added, the faster the dielectric constant and  $Q \times f$  value decrease. The main cause comes from the lower dielectric constant and large dielectric loss of LBS. The ceramic can be sintered well at low sintering temperature and is mainly attributed to the presence of a liquid phase, which fills the gaps between powders, lubricates powders, and forms a capillary membrane, which together accelerate the rearrangement behavior of powders and forms a compact structure.

## ACKNOWLEDGMENTS

This work is supported by the National Natural Science Foundation of China (No. 51272035) and Specialized Research Fund for the Doctoral Program of Higher Education of China (No. 20110185120004).

## ORCID

Hongyu Yang  <http://orcid.org/0000-0002-5894-1693>

## REFERENCES

1. Zhou J. Towards rational design of low-temperature co-fired ceramic (LTCC) materials. *J Adv Ceram.* 2012;1:89-99.
2. Sebastian MT. *Dielectric Materials for Wireless Communication.* Amsterdam, the Netherlands: Elsevier; 2008:1-671.
3. Zhou MZ, Jean JH. Low-fire processing of microwave  $\text{BaTi}_4\text{O}_9$  dielectric with  $\text{BaO-ZnO-B}_2\text{O}_3$  glass. *J Am Ceram Soc.* 2006;89:786-791.
4. Choy JH, Han YS, Hwang SH, et al. Citrate Route to Sn-Doped  $\text{BaTi}_4\text{O}_9$  with Microwave Dielectric Properties. *J Am Ceram Soc.* 1998;81:3197-3204.
5. Fu MS, Liu XQ, Chen XM, et al. Effects of Mg Substitution on Microstructures and Microwave Dielectric Properties of  $\text{Ba}(\text{Zn}_{1/3}\text{Nb}_{2/3})\text{O}_3$  Perovskite Ceramics. *J Am Ceram Soc.* 2010;93:787-795.
6. Lee CC, Chou CC, Tsai DS. Effect of La/K A-site Substitutions on the Ordering of  $\text{Ba}(\text{Zn}_{1/3}\text{Ta}_{2/3})\text{O}_3$ . *J Am Ceram Soc.* 1997;80:2885-2890.
7. Sebastian MT, Jantunen H. Low loss dielectric materials for LTCC applications: a review. *Int Mater Rev.* 2008;53:57-90.
8. Zhou D, Dou G, Guo M, et al. Low temperature sintering and microwave dielectric properties of  $\text{ZnTiNb}_2\text{O}_8$  ceramics with  $\text{BaCu}(\text{B}_2\text{O}_5)$  additions. *Mater Chem Phys.* 2011;130:903-908.
9. Zhou D, Pang LX, Guo J, et al. Phase evolution, phase transition, raman spectra, infrared spectra, and microwave dielectric properties of low temperature firing  $(\text{K}_{0.5x}\text{Bi}_{1-0.5x})(\text{Mo}_x\text{V}_{1-x})\text{O}_4$  ceramics with scheelite related structure. *Inorg Chem.* 2011;50:12733-12738.
10. Zhou D, Pang LX, Guo J, et al. Influence of Ce substitution for Bi in  $\text{BiVO}_4$  and the impact on the phase evolution and microwave dielectric properties. *Inorg Chem.* 2014;53:1048-1055.
11. Zhou D, Fan XQ, Jin XW, et al. Structures, Phase Transformations, and Dielectric Properties of  $\text{BiTaO}_4$  Ceramics. *Inorg Chem.* 2016;55:11979-11986.
12. Zhou D, Guo D, Li WB, et al. Novel temperature stable high- $\epsilon_r$  microwave dielectrics in the  $\text{Bi}_2\text{O}_3\text{-TiO}_2\text{-V}_2\text{O}_5$  system. *J Mater Chem C.* 2016;4:5357-5362.
13. Zhou D, Pang LX, Wang DW, et al. High permittivity and low loss microwave dielectrics suitable for 5G resonators and low temperature co-fired ceramic architecture. *J Mater Chem C.* 2017;5:10094-10098.
14. Baumgarte A, Blachnik R. New  $\text{M}^{2+}\text{M}^{4+}\text{Nb}_2\text{O}_8$  phases. *J Alloy Compd.* 1994;215:117-120.
15. Kim D, Kim D, Hong KS. Phase relations and microwave dielectric properties of  $\text{ZnNb}_2\text{O}_6\text{-TiO}_2$ . *J Mater Res.* 2000;15:1331-1335.
16. Bafrooei HB, Nassaj ET, Ebadzadeh T, et al. Sintering behavior and microwave dielectric characteristics of  $\text{ZnTiNb}_2\text{O}_8$  ceramics achieved by reaction sintering of  $\text{ZnO-TiO}_2\text{-Nb}_2\text{O}_5$  nanosized powders. *Ceram Int.* 2016;42:3296-3303.
17. Li K, Wang H, Zhou H, et al. Silver Co-Firable  $\text{ZnTiNb}_2\text{O}_8$  Microwave Dielectric Ceramics with  $\text{Li}_2\text{O-ZnO-B}_2\text{O}_3$  Glass Additive. *Int J Appl Ceram Technol.* 2010;7:E144-E150.
18. Tseng CF, Chen PH, Lin PA. Low temperature sintering and microwave dielectric properties of  $\text{Zn}_{0.5}\text{Ti}_{0.5}\text{NbO}_4$  ceramics with ZnO additive for LTCC applications. *J Alloy Compd.* 2015;632:810-815.

19. Li E, Niu N, Wang J, et al. Effect of Li–B–Si glass on the low temperature sintering behaviors and microwave dielectric properties of the Li-modified ss-phase  $\text{Li}_2\text{O–Nb}_2\text{O}_5\text{–TiO}_2$  ceramics. *J Mater Sci Mater Electron*. 2015;26:3330-3335.
20. Rietveld HM. A profile refinement method for nuclear and magnetic structures. *J Appl Crystallogr*. 2010;2:65-71.
21. Takahiro T, Wang SF, Shoko Y, et al. Effect of Glass Additions on BaO–TiO<sub>2</sub>–WO<sub>3</sub> Microwave Ceramics. *J Am Ceram Soc*. 1994;77:1909-1916.
22. Tseng CF. Microwave dielectric properties of low loss microwave dielectric ceramics:  $\text{A}_{0.5}\text{Ti}_{0.5}\text{NbO}_4$  (A = Zn, Co). *J Eur Ceram Soc*. 2014;34:3641-3648.
23. Valant M, Suvorov D, Pullar RC, et al. A mechanism for low-temperature sintering. *J Eur Ceram Soc*. 2006;26:2777-2783.
24. Singh VK. Densification of Alumina and Silica in the Presence of a Liquid Phase. *J Am Ceram Soc*. 1981;64:C-133-C-136.
25. Funahashi S, Guo J, Guo H, et al. Demonstration of the cold sintering process study for the densification and grain growth of ZnO ceramics. *J Am Ceram Soc*. 2017;100:546-553.
26. Cahn JW, Heday RB. Analysis of Capillary Forces in Liquid-Phase Sintering of Jagged Particles. *J Am Ceram Soc*. 1970;53:406-409.
27. Baumgarte A, Blachnik R. Phase relations in the system titanium-dioxide-diniobium-zinc-hexoxide. *Mater Res Bull*. 1992;27:1287-1294.
28. Shannon RD. Dielectric polarizabilities of ions in oxides and fluorides. *J Appl Phys*. 1993;73:348-366.
29. Guo J, Berbano SS, Guo H, et al. Cold Sintering Process of Composites: bridging the Processing Temperature Gap of Ceramic and Polymer Materials. *Adv Func Mater*. 2016;26:7115-7121.
30. Kim ES, Chun BS, Freer R, et al. Effects of packing fraction and bond valence on microwave dielectric properties of  $\text{A}^{2+}\text{B}^{6+}\text{O}_4$  ( $\text{A}^{2+}$ : Ca, Pb, Ba;  $\text{B}^{6+}$ : Mo, W) ceramics. *J Eur Ceram Soc*. 2010;30:1731-1736.
31. Shannon RD. Revised effective ionic radii and systematic studies of interatomic distances in halides and chalcogenides. *Acta Crystallogr A*. 1976;32:751-767.

**How to cite this article:** Yang H, Li E, Yang H, He H, Zhang RS. Synthesis of  $\text{Zn}_{0.5}\text{Ti}_{0.5}\text{NbO}_4$  microwave dielectric ceramics with  $\text{Li}_2\text{O–B}_2\text{O}_3\text{–SiO}_2$  glass for LTCC application. *Int J Appl Glass Sci*. 2017;00:1-11. <https://doi.org/10.1111/ijag.12334>